Emission spectroscopy of clay minerals and evidence for poorly crystalline aluminosilicates on Mars from Thermal Emission Spectrometer data

Joseph R. Michalski,[1] Michael D. Kraft,[1] Thomas G. Sharp,[1] Lynda B. Williams,[1] and Philip R. Christensen[1]

Received 23 March 2005; revised 13 October 2005; accepted 21 November 2005; published 14 March 2006.

[1] To understand the aqueous history of Mars, it is critical to constrain the alteration mineralogy of the Martian surface. Previously published analyses of thermal infrared (λ = 6–25 μm) remote sensing data of Mars suggest that dark regions have ~15–20% clay minerals. However, near-infrared (λ = 1–3 μm) spectral results generally do not identify widespread clay minerals. Thermal infrared detections of clays on Mars are difficult to interpret owing in part to the relative paucity of published spectral analyses of clay minerals and clay-bearing materials using similar spectra (thermal infrared emission spectra). In this study, we present an analysis of the thermal emission spectral features (λ = ~6–25 μm or 400–1650 cm^{-1}) of a suite of clay mineral reference materials and clay-bearing rocks, linking their spectral features to the crystal chemical properties of the clays. On the basis of this context provided by the emission spectral analysis of clay minerals and clay-bearing rocks, we reconsider the evidence for clay minerals on Mars from Thermal Emission Spectrometer (TES) results. We propose that global-scale clay abundances determined from TES probably represent a geologically significant surface component, though they may actually correspond to poorly crystalline aluminosilicates with similar Si/O ratios to clay minerals (0.3–0.4), rather than well-crystalline clays. If clay minerals or clay-like materials on Mars are poorly crystalline and/or dessicated, they may be detectable in the thermal infrared, but not easily detected with near-infrared data sets.

Citation: Michalski, J. R., M. D. Kraft, T. G. Sharp, L. B. Williams, and P. R. Christensen (2006), Emission spectroscopy of clay minerals and evidence for poorly crystalline aluminosilicates on Mars from Thermal Emission Spectrometer data, *J. Geophys. Res.*, *111*, E03004, doi:10.1029/2005JE002438.

1. Introduction

[2] In this manuscript, we report the results of a laboratory analysis of the thermal emission spectral properties of clay minerals and we consider the spectral evidence for clay minerals on Mars from Thermal Emission Spectrometer (TES) surface spectra. The spectral identification and analysis of clay minerals is critical to understanding lithologies and chemical weathering of geological materials from thermal infrared remote sensing analyses. On Mars, there is abundant evidence for present-day water [*Feldman et al.*, 2002, 2004], past aqueous geomorphic systems [*Baker et al.*, 1992; *Carr*, 1996; *Malin and Edgett*, 2000a; *Mustard et al.*, 2001; *Malin and Edgett*, 2003; *Christensen*, 2003], diverse and wide-spread sedimentary deposits [*Malin and Edgett*, 2000b, 2001, 2003; *Edgett and Malin*, 2002; *Tanaka et al.*, 2003; *Squyres et al.*, 2004], magma-ice interactions [*Chapman*, 2003; *Fagents et al.*, 2003], and impact into ice-rich terrains [*Squyres et al.*, 1992], suggesting that hydrous secondary phases may be important components of the Martian geologic record. The observation of hydrogen, even at low Martian latitudes where ice is likely unstable, suggests that weakly hydrated secondary phases are probably present at the Martian surface [*Feldman et al.*, 2002; *Fialips et al.*, 2005], and clay minerals are a possible candidate. However, if Mars was only episodically wet or chemically weathered under dry and cold conditions, amorphous or poorly ordered silicate alteration products might be favored over clay minerals as chemical weathering products [*Gooding et al.*, 1992].

[3] Remote sensing results provide a test for the question of clay occurrences on Mars. Previous spectral analyses of Mars using visible/near-infrared spectra (VNIR) (λ = 0.5–3 μm) have not shown clay minerals to be widespread and abundant [*Singer et al.*, 1979; *McCord et al.*, 1982; *Soderblom*, 1992; *Murchie et al.*, 1993; *Beinroth and Arnold*, 1996; *Bell et al.*, 1997; *Murchie et al.*, 2000; *Bibring et al.*, 2005; *Mustard et al.*, 2005]. Recent results from the Mars Express OMEGA Experiment have shown that clay minerals occur locally in a limited number of places, but are not observed at regional or global scales on

[1]Department of Geological Sciences, Arizona State University, Tempe, Arizona, USA.

0148-0227/06/2005JE002438$09.00

Mars [*Bibring et al.*, 2005; *Mustard et al.*, 2005]. Thermal infrared (λ = ~6–25 μm or 400–1650 cm^{-1}) TES data have been used to constrain the global surface mineralogy of Mars (at spatial scales of ~1000s of km^2), including clay mineral abundances, from linear spectral deconvolution of global spectral surface types. Most TES studies report some component of clay minerals in linear spectral deconvolution results [*Bandfield et al.*, 2000; *Christensen et al.*, 2000a; *Hamilton et al.*, 2001; *Christensen et al.*, 2001; *Bandfield*, 2002; *Wyatt and McSween*, 2002; *Rogers and Christensen*, 2003; *McSween et al.*, 2003; *Minitti et al.*, 2002], but the meaning of clay abundances returned from spectral deconvolution of TES data has been debated. The problem is complicated by the lack of published, detailed spectral analyses discussing the emission spectra of clay minerals. This is important because the spectral features of clay minerals that cause them to fit into a TES spectral model could potentially be shared by other minerals, but this is difficult to evaluate without background research linking the spectral features of clays to their mineralogical properties. In addition, it is not clear whether the linear spectral deconvolution approach used to analyze TES data provides meaningful results with regard to clay abundances (compared with other mineral groups).

[4] It is possible that linear spectral deconvolution produces accurate abundances of clay minerals in altered rocks, but this has not been demonstrated. The linear spectral deconvolution technique employs a least squares minimization algorithm to model observed emissivity spectra with an input library of spectra [*Ramsey and Christensen*, 1998]. The fundamental assumption in linear spectral modeling is that spectral features of a mixed scene are in fact a result of the linear spectral combination of the spectra of separate, distinct phases within that scene. Linear deconvolution has been rigorously tested on mineral particulate mixtures [*Ramsey and Christensen*, 1998], igneous rocks [*Hamilton et al.*, 1997; *Ruff*, 1998; *Feely and Christensen*, 1999; *Wyatt et al.*, 2001; *Michalski et al.*, 2004], and metamorphic rocks [*Feely and Christensen*, 1999], but never on sedimentary rocks and rarely on altered, clay-rich rocks [*Christensen and Harrison*, 1993; *Michalski et al.*, 2004]. In the case of metamorphic rocks, *Feely and Christensen* [1999] reported difficulty in modeling abundances of phyllosilicates (mostly micas). On theoretical grounds, it is possible that clay minerals could be more difficult to model using this technique than other mineral groups. One of the assumptions in linear spectral deconvolution is that intimately mixed minerals have thicknesses greater than their optical thicknesses (~40–60 μm for silicates [*Ramsey and Christensen*, 1998]). Clay minerals can occur as coarse particulates in some cases, but commonly the size of clay crystals or aggregates of clay crystals in rocks and soils is $\ll$40 μm. Therefore photons emitted from individual phases in a clay-bearing mixture may interact with more than one phase before reaching the detector, resulting in nonlinear spectral mixing. It is important to test the linear spectral deconvolution approach on TES-like thermal infrared spectra of clay-bearing materials on Earth, to help understand the meaning of modeled results at Mars.

[5] This paper is an attempt to deal with some of the complications of interpreting clay mineral abundances from TES spectra and to reconcile their potential detection with lack of evidence for clays in VNIR data by linking the thermal emission spectral properties of clay minerals to their crystal chemistry. Section 2 of the manuscript contains background information about clay minerals and infrared spectroscopy. Thermal emission spectra of clay minerals are presented in section 3, including spectra from previous studies and new spectra of clay reference materials. In that section, the relationships of infrared spectral absorptions to the mineralogical properties of clay minerals are discussed. The assumption of linear spectral mixing of clay minerals in thermal emission spectra of clay-rich rocks is tested and discussed in section 4. In section 5, we discuss the geological implications of TES analyses of clay minerals on Mars.

2. Background and Methods

2.1. Basic Clay Mineralogy

[6] Clay minerals are phyllosilicates that commonly have crystal sizes <2 μm in average dimensions, though some clay minerals can be coarsely crystalline. The structure of clay minerals can be discussed in terms of "sheets" and "layers." Two types of sheets occur in clay minerals, octahedrally coordinated sheets (O) and tetrahedrally coordinated sheets (T). The sheets are stacked together to form TO or TOT layers. The T sheets consist of TO_4 tetrahedra where the T cation (T = Si^{4+}, Al^{3+}, and Fe^{3+}) exists in fourfold coordination with O^{2-} anions. The Si/O ratio of the tetrahedral layer in phyllosilicates varies from 0.3 to 0.4, depending on the amount of Al^{3+} and Fe^{3+} substitution for Si^{4+} in the tetrahedral sites. The O sheets consist of M-$(O,OH)_6$ octahedra (predominantly, M = Al^{3+}, Fe^{3+}, Fe^{2+}, and Mg^{2+}), where M cations exist in 6-fold coordination with O^{2-} and OH^- anions. If the M cations are divalent, all of the octahedral sites are filled and the clay is considered trioctahedral. If the M cations are trivalent, only two thirds of the octahedral sites are filled and it is called dioctahedral. In reality, both divalent and trivalent cations are commonly present; clays are commonly considered dominantly trioctahedral (e.g., saponite) or dioctahedral (e.g., nontronite). When the net charge balance of the TOT sheets is negative owing to cation substitutions (termed "layer charge"), large cations such as K^+, Na^+, or Ca^+ can occur in interlayer sites between TOT layers to achieve charge balance [*Moore and Reynolds*, 1997]. Clay minerals are classified according to: (1) their structure (TO, e.g., kaolinite, versus TOT, e.g., montmorillonite), (2) the dioctahedral or trioctahedral nature of octahedral sheets, and (3) their degree of expandability (which is high for clays with small layer charge, low for clays with high layer charge, and essentially zero for clays with no appreciable layer charge). Clay minerals can also occur as mixed-layer varieties, the most common of which is mixed-layer illite-smectite (I/S) [*Hower and Mowatt*, 1966]. During diagenesis, smectite clays recrystallize to illite; therefore the degree of illitization is a reflection of the degree of diagenetic recrystallization that smectite-bearing sediments have experienced, as a function of temperature and pressure.

2.2. Previous Studies of Clay Spectroscopy

[7] The application of spectroscopy as an analytical tool has become commonplace in the study of clay minerals.

Most recent spectroscopic analyses of clay minerals deal with specific problems in clay mineralogy, and there are too many to cite properly. We are concerned with understanding the relationship of emission spectral features to basic clay mineralogy for the purpose of remote geological studies, and as such, we point the reader to many early references on the subject of clay spectroscopy, which discuss these basic relationships. The foundation for our spectral interpretations, the relation of certain spectral features to specific crystal chemical properties, comes from these references. Many previous studies have demonstrated the use of infrared transmission [e.g., *Keller and Pickett*, 1950; *Launer*, 1952; *Farmer*, 1958; *Brindley and Zussman*, 1959; *Stubican and Roy*, 1961a, 1961b; *Farmer and Russell*, 1964; *Farmer*, 1974] (and reviews by *Madejová* [2003], *Gates* [2005], *Madejová and Komadel* [2005], and *Petit* [2005]) or reflection spectroscopy [e.g., *Hunt and Salisbury*, 1970; *Hunt et al.*, 1973; *Abrams et al.*, 1977; *Hunt and Ashley*, 1979; *Hunt and Evarts*, 1981; *Hunt and Hall*, 1981; *Goetz et al.*, 1983; *Mustard and Pieters*, 1987; *Lang et al.*, 1990; *Bishop et al.*, 1993, 1994, 1998; *Bishop*, 2002; *Bishop et al.*, 2002] for mineralogical studies. Transmission spectra, despite containing similar spectral information, are not easily applied to analysis of infrared remote sensing data; therefore it is necessary to study the emission spectra of materials for comparison with thermal infrared remote sensing data. There have been published reports of emission analyses of clay minerals [*Kloprogge et al.*, 2000; *Kloprogge and Frost*, 2005], but this terminology is a misnomer with respect to traditional spectroscopy and remote sensing literature. *Kloprogge et al.* [2000] mixed terminology for radiance and emissivity and measured the emission of sample cups through thin clay films on the cups, which by common definition is a transmission measurement. Various authors have dealt with the emission spectra of clay-bearing materials [e.g., *Christensen and Harrison*, 1993; *Roush and Orenberg*, 1996; *Piatek*, 1997; *Stefanov*, 2000; *Michalski et al.*, 2005], but none of these studies focused on the emission spectral features of relatively pure clay minerals and their relationship to mineralogical properties. *Piatek* [1997] published the first analysis of the emission spectral features of clay minerals, but that study had some limitations: (1) The clays used were impure; particle size separation was not performed on the clay reference materials, which is necessary in order to minimize the impurities present in the samples. (2) As a result, spectra produced in that study have some spectral features which seemingly correspond to impurities. (3) Although samples were characterized by X-ray diffraction (XRD), the diffraction studies were not performed by standard practices for analysis of clay-bearing materials (refer to *Moore and Reynolds* [1997]), which results in difficulty characterizing the samples used. (4) No standard physical sample preparation was utilized, and as a result, it is not clear which features of the clay spectra are a result of physical variability between samples or mineralogical variability. (5) Spectral features of clay minerals were analyzed by structure type (TO versus TOT, etc.), but not related to the crystal chemistry of the samples used. (6) Spectral features are misinterpreted in some cases. Although Piatek's study provided spectra that are widely used in the planetary community in the analysis of spectral data from TES, the uncertainties surrounding that spectral study contribute in part to uncertainties in interpreting clay detections on Mars with the TES data.

[8] In a previous study, we discussed the emission spectral features of smectite clay minerals [*Michalski et al.*, 2005], but that study was focused on the topic of silica-rich materials observed on Mars. In that work, the question of whether clay minerals could satisfy the observation of a silica-rich surface component observed at Mars in TES data was addressed. This work differs from that study in several ways. In this study, we (1) extend the previous work to discuss spectra of several of the most common clay minerals on Earth and provide a more comprehensive analysis of emission spectral features of diverse clay minerals, (2) discuss the spectral features of clay-bearing rocks, and (3) specifically address the topic of clay mineral abundances on Mars from TES data, aside from the topic of high-silica materials.

2.3. Sample Geology, Characterization, and Preparation

[9] Here we compare the emission spectra of smectite clay minerals from *Michalski et al.* [2005] with emission spectra of kaolinite, halloysite, serpentine, illite, and illite/smectite (I/S) mixed layer clay. All samples, except where otherwise noted, are from the Clay Minerals Society (CMS) repository and have been well characterized previously [*Post et al.*, 1997; *Keeling et al.*, 2001; *Borden and Giese*, 2001; *Chipera and Bish*, 2001; *Guggenheim and Koster Van Groos*, 2001; *Kogel and Lewis*, 2001; *Madejová and Komadel*, 2001; *Mermut and Cano*, 2001; *Moll*, 2001; *Wenju*, 2001]. The saponite and serpentine were characterized by *Eberl et al.* [1982] and *Piatek* [1997], respectively. To minimize impurities present in our samples of the reference clays, we separated out the fine-size fractions (either <0.2 or <2 μm) [Table 1]. The coarse-size fraction (>710 μm) of serpentine (antigorite) was used because this mineral was available in coarsely crystalline form with adequate purity. To supplement previous characterization, we carried out additional XRD analyses and thermal infrared transmission spectroscopy (KBr pellet technique, commonly referred to simply as "FTIR") on each sample. Details of the preparation and characterization procedure are reported by *Michalski et al.* [2005].

[10] In addition to spectra of relatively pure clay reference materials, we analyzed the emission spectral features of heterogeneous clay-bearing rocks (mudstones). Mudstone samples were collected near Walsenburg, Colorado. The mudstones are from the Cretaceous Pierre Shale where a mafic dike intruded the mudstone causing illitization of smectite clays in a contact aureole around the dike [*Pytte*, 1982; *Lynch*, 1985; *Williams et al.*, 2001]. The mudstone samples were characterized by XRD of both the bulk rock powders and the clay-size fractions.

2.4. Emission Spectroscopic Methods

[11] Emission spectra of clay mineral standards and rock samples were acquired at Arizona State University (ASU) using a Nicolet Nexus 670 spectrometer, which has been modified to measure emitted energy, rather than transmitted energy. The instrument setup and calibration

Table 1. Characteristics of Clay Minerals Used in This Study[a]

Name	Sample Number	Source	Size Fraction	Structural Formula	Si/O ratio	Al/Si ratio
Nontronite[b]	NAu-1	CMS	<0.2 μm	$(Al_{0.15}Fe_{1.84}Mg_{0.02})(Al_{0.51}Si_{3.49})O_{10}(OH)_2$	0.349	0.15
Montmorillinite[c]	SWy-1	CMS	<0.2 μm	$(Fe_{0.21}Al_{1.51}Mg_{0.27}Ti_{0.01})(Al_{0.01}Si_{3.99})O_{10}(OH)_2$	0.399	0.00
Beidellite[d]	SBdl-1	CMS	<0.2 μm	$(Fe^{3+}{}_{0.10}Al_{1.79}Mg_{0.05}Ti_{0.05})(Al_{0.23}Si_{3.77})O_{10}(OH)_2$	0.377	0.06
Hectorite[e]	SHCa-1	CMS	<0.2 μm	$(Li_{0.7}Mg_{2.3}Ti_{0.01})(Fe_{0.03}Al_{0.09}Si_{3.88})O_{10}(OH)_2$	0.388	0.02
Saponite[e]	SpNv-1	D. E.[4]	<0.2 μm	$(Li_{0.09}Mg_{2.72}Fe^{3+}{}_{0.03}Al_{0.07})(Al_{0.04}Si_{3.96})O_{10}(OH)_2$	0.396	0.01
Kaolinite	KGa-1	CMS	<2.0 μm	$(Al_{1.94}Ti_{0.05}Fe_{0.01})(Si_{1.93}Al_{0.07})O_5(OH)_4$	0.386	0.04
Halloysite	HWw-1	Ward's	<0.2 μm	$Ca_{0.01}Na_{0.02}(Al_{1.95}Fe_{0.05})(Si_{1.96}\ Al_{0.04})O_5(OH)_4$	0.392	0.02
Serpentine	BUR-1690	Burminco	>710 μm	$(Mg_{2.8}Fe_{.35})(Si_{1.87}Al_{0.07})O_5(OH)_4$[†]	0.374	0.04
Illite	Imt-1	CMS	<0.2 μm	$Mg_{0.04}Ca_{0.03}K_{0.87}(Al_{1.45}Fe^{3+}{}_{0.38}Fe^{2+}{}_{0.03}Mg_{0.22}Ti_{0.03})(Si_{3.37}Al_{0.62})O_{10}(OH)_2$	0.337	0.18
Illite-Smectite mixed layer 60/40	ISMt-1	CMS	<2.0 μm	$Mg_{0.03}Ca_{0.1}K_{0.42}(Al_{1.68}Fe^{3+}{}_{0.08}Fe^{2+}{}_{0.01}Mg_{0.23}Ti_{0.01})(Si_{3.54}Al_{0.46})O_{10}(OH)_2$	0.354	0.13

[a]Interlayer chemistry is not reported for smectites because they were k-saturated.
[b]*Keeling et al.* [2000].
[c]*Mermut and Cano* [2001].
[d]*Post et al.* [1997].
[e]*Eberl et al.* [1982] and *Khoury et al.* [1982].

procedure for a similar spectrometer that previously existed in this laboratory are described by *Christensen and Harrison* [1993] and *Ruff et al.* [1997]. A description of the spectrometer instrument setup used to collect spectra of clay pellets is discussed by *Michalski et al.* [2005]. Rock spectra were collected using the instrument settings discussed by *Michalski et al.* [2004].

[12] Thermal infrared spectra of the mudstones were analyzed quantitatively using a linear spectral deconvolution technique developed by *Ramsey and Christensen* [1998]. The input library used for this analysis consisted of 15 endmembers, including a range of feldspar compositions (microcline, orthoclase, albite, oligoclase, and andesine), quartz (both coarsely crystalline and microcrystalline), clay minerals (illite, montmorillonite, I/S, and kaolinite) and a blackbody component to account for differences in spectral contrast that are unrelated to composition. The deconvolution algorithm was applied to the spectral range from 350 to 1400 cm^{-1}. The results of linear spectral deconvolution are considered reliable to ±10% abundance (by volume) for most igneous minerals based on empirical data [*Feely and Christensen*, 1999].

2.5. XRD Methods

[13] We performed XRD on the clay standards and rock samples using a Siemens D-5000 X-ray diffractometer with Cu-Kα radiation. Clay mineral standards were analyzed as oriented slide mounts of the finest size fraction (Table 1) according to methods described by *Moore and Reynolds* [1997]. XRD analysis was performed on the mudstones in two steps. The first phase involved identification of individual phases by peak matching of the bulk powder XRD patterns using Jade® software. The second phase involved quantification of known mineral abundances using the RockJock program developed by *Eberl* [2003]. Each rock was gently ground into a powder and passed through a 45-μm sieve. Each powder was side loaded and gently packed into a disk-shaped (∼1 cm thick × ∼2 cm diameter) sample holder; the top of the disk was then removed to collect diffraction data from the upper portion of the packed powder. Data were collected from 5–65° 2θ, in 0.2° steps. Quantitative analyses include modeling of bulk powder XRD data using the methods described by *Środoń et al.* [2001]. The modeling process is an interactive process by which the library input was selected (on the basis of a priori information) to provide a reasonable fit. By "reasonable fit," we mean unconstrained totals close to 100% (±5%). In this case, the library input included albite, microcline, illite, I/S mixed layer clay, montmorillonite, quartz, and kaolinite. In presenting the results, we group the abundances of the members of each mineral group into total clay, total feldspar, and quartz. Reported errors for this technique are <5% absolute abundance for each phase for artificial mixtures, but difficult to determine for natural samples [*Środoń et al.*, 2001]. We acknowledge that errors could be >5% for our samples, but consider unconstrained sums of close to 100% to be an indication that modeling results are accurate. Weight percent abundances determined by XRD modeling were converted to volume modes using approximate mineral densities for comparison to abundances

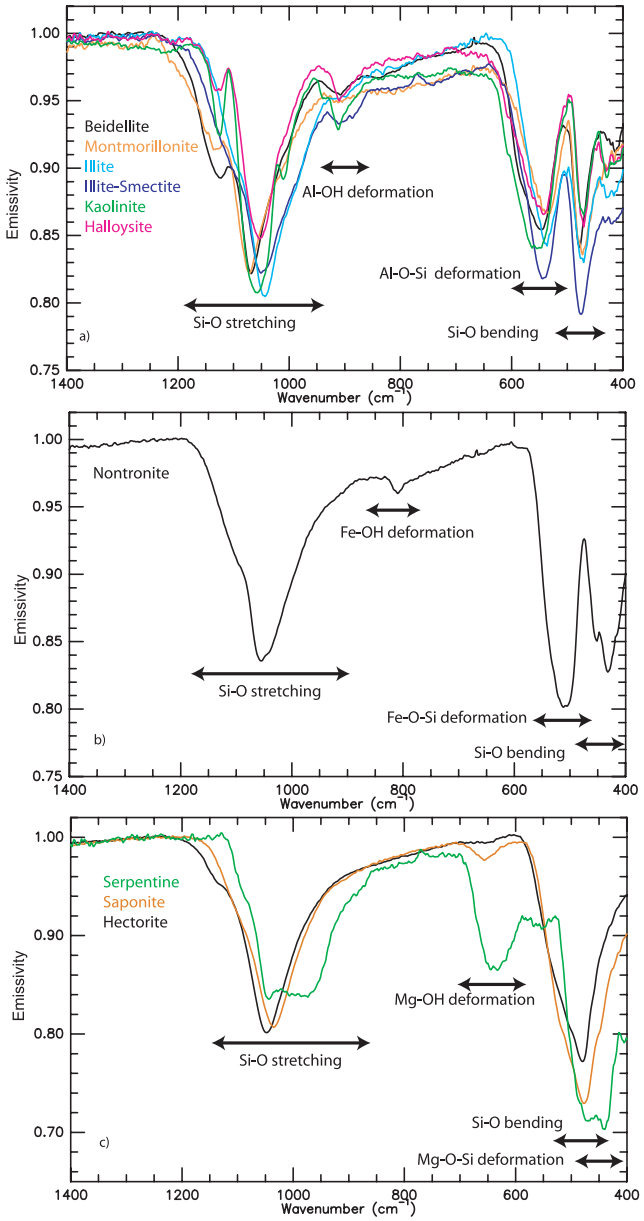

Figure 1. Thermal infrared emission spectra of all clay pellets. The clays are grouped by spectral and crystal chemical similarity into (a) aluminous clays, (b) ferruginous clay, and (c) magnesian clays.

determined by linear deconvolution of thermal emission spectra.

3. Emission Spectra of Clay Minerals

3.1. Tetrahedral and Octahedral Sheets

[14] Thermal infrared emission spectra of clay minerals have absorptions corresponding to the various bonds within the structure. Absorptions related to (Si,Al)-O stretching in the tetrahedral sheets occur between 900 and 1300 cm^{-1} [*Keller and Pickett*, 1950] and are centered near 1050 cm^{-1}. Between 500 and 930 cm^{-1}, librational (rotational vibration) absorptions correspond to M-OH bonds in the octahedral sheets [*Farmer*, 1958; *Brindley and Zussman*, 1959; *Stubican and Roy*, 1961a]. The M-O-Si bonds between octahedral and tetrahedral sheets absorb between 450 and 550 cm^{-1} [*Stubican and Roy*, 1961a; *Farmer*, 1974]. Si-O bending absorptions corresponding to the tetrahedral sheet occur near 470 cm^{-1}. M-O bonds absorb between 250 and 450 cm^{-1} and interlayer cations absorb at <200 cm^{-1} [*Farmer*, 1974]. Thermal infrared emission spectra of all of the pelletized samples are shown in Figure 1. As a group, the clay minerals all have Si-O stretching absorptions centered between 1000 and 1100 cm^{-1}. All of the clay minerals have molar Si/O ratios between 0.3 and 0.4, intermediate between that of the most polymerized silicates (quartz, Si/O = 0.5) and the most depolymerized silicates (e.g., olivine, Si/O = 0.25). As a result, the clay minerals exhibit Si-O stretching absorptions at an intermediate energy between those of tectosilicates and nesosilicates. Within the clay minerals the exact placement of the Si-O stretching absorption is a complex function of the chemistry of the tetrahedral sheet and the symmetry of the crystal structure. Substitution of Al^{3+} for Si^{4+} into the tetrahedral sheets shifts the Si-O stretching absorption to lower wave numbers. However, this is not a simple linear relationship as a function of tetrahedral sheet chemistry; the Si-O stretching absorption of trioctahedral clay minerals occurs at lower wave numbers than that of dioctahedral clay minerals. This occurs because some of the tetrahedral O^{2-} anions are bonded to the octahedral cations, and therefore, Si-O tetrahedra are affected by the identity of octahedral cations. Absorptions related to Si-O bending in the tetrahedral sheets of our samples occur near 470 cm^{-1}.

[15] Absorptions related to the octahedral sheets and bonds between the octahedral and tetrahedral sheets occur between 300 and 950 cm^{-1}. The placement of M-OH (predominantly, M = Al^{3+},Fe^{3+}, Fe^{2+}, and Mg^{2+}) absorptions is a function of the bond strength and is related to ionic radius and charge of the M-cation. For each clay mineral, individual absorptions are present that are related to each of the octahedral cation species; these are observed in transmission spectra, which are highly sensitive to even minor absorptions (Figure 2). However, on the basis of this

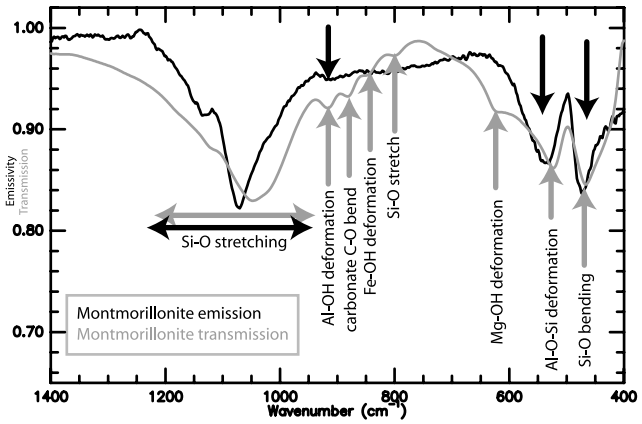

Figure 2. Comparison of the thermal infrared emission spectrum and thermal infrared transmission spectrum of montmorillonite (SWy-1). Gray arrows point to absorptions present in the transmission spectrum; black arrows identify the same absorptions in emission. Minor absorptions are easily observed in the transmission spectrum, but not in the emission spectrum.

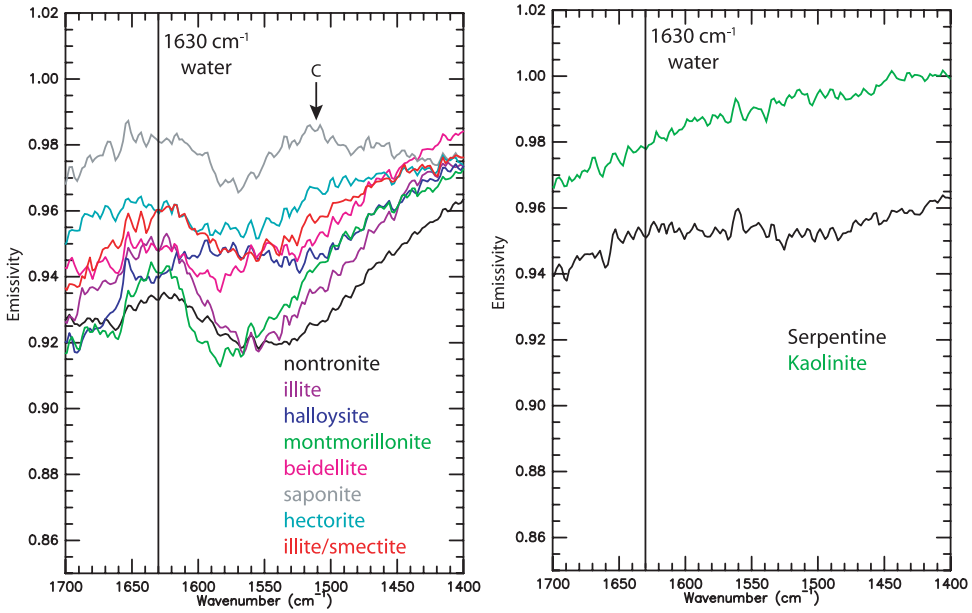

Figure 3. Thermal emission spectra of clay powders showing the presence of a water feature at 1630 cm^{-1} in the TOT clays and halloysite, but an absence of the water feature in the TO clays, serpentine, and kaolinite. "C" corresponds to a minor carbonate absorption in the saponite sample.

analysis, emission spectra of clays do not appear to have the sensitivity to identify absorptions related to each cation vibration in the octahedral sheet. Only the most abundant octahedral cations produce significant absorptions in the emission spectra. This is not a problem for identifying the major crystal chemical features of clay minerals; most clay minerals are dominantly aluminous, ferruginous, or magnesian. In each of these cases, the absorptions related to Al-OH, Fe-OH, or Mg-OH can be resolved. However, in a dominantly aluminous clay mineral, the Mg-OH absorption related to a minor Mg-component in the octahedral sheet is not resolvable with emission spectroscopy.

[16] The absorption in the 490–550 cm^{-1} region of spectra of dioctahedral clay minerals results from the M^{3+}-O-Si bonds between the dioctahedral and tetrahedral sheets [*Stubican and Roy*, 1961a; *Farmer*, 1974]. Whereas the frequencies of M-OH absorptions appear to be cation-specific, the frequency of the M-O-Si absorption appears to be a linear function of the average ionic radius of the cation(s) in the octahedral site [*Stubican and Roy*, 1961a; *Michalski et al.*, 2005]. The M^{2+}-O-Si bonds in trioctahedral minerals absorb at lower energies than that of dioctahedral minerals and overlap with the Si-O bending absorption in the tetrahedral sheet. As a result, the absorption related to Mg^{2+}-O-Si deformation in trioctahedral smectites is not uniquely identifiable in emission spectra.

3.2. Effects of Interlayer Cations and Interlayer Water

[17] Absorptions related to the interlayer cations (such as Na^{+}, Ca^{2+}, K^{+}, and Mg^{2+}) are of low energy and therefore occur at low wave numbers (<250 cm^{-1}) [*Farmer*, 1974]. This spectral range is accessible with Raman spectroscopic techniques, but is not easily accessible by thermal emission or reflection techniques. Therefore it is not currently possible to determine the interlayer chemistry of clay minerals from thermal infrared remote sensing data.

[18] The transmission spectra of all of our clay samples show evidence for the presence of interlayer water with minor absorptions near 1630 cm^{-1}. However, the emission spectra of pressed clay pellets do not show this absorption. The most likely explanation is that the emission spectra of indurated samples are less sensitive to minor absorptions, such as the bound water absorption near 1630 cm^{-1}. By contrast, the emission spectra of powdered clay samples do show evidence for hydration in some cases (Figure 3). The nonlinear spectral effects that result from small particle sizes make some minor spectral components visible in the powdered spectra that are not present in the spectra of pressed pellets. While none of the pellet spectra show evidence for interlayer water at 1630 cm^{-1}, the water band is observed in powder spectra of all of the TOT clays and halloysite. The spectra of serpentine and kaolinite powders, which have essentially zero interlayer water, show no spectral evidence for interlayer water. We acknowledge that equilibration of the clays with the atmosphere during pellet pressing and during spectral analysis likely resulted in changes in the hydration state of the clays. However, because we are unconcerned with quantifying the amount of water in the clays, we do not consider this to be a problem.

3.3. Orientation Effects

[19] The pressed clay pellets used in this study may have preferred orientations from compression. To test whether spectral differences could arise due to the orientation of crystals in the pellets, the pellets were cut in half and spectra were recorded from an edge-on view. Emission from the normal and edge-on views of the clay pellets produced no significant spectral differences for either trioctahedral or dioctahedral clay minerals, suggesting that either (1) the clay crystals were not significantly oriented during pressing or (2) the optical axes of triclinic an monoclinic clay

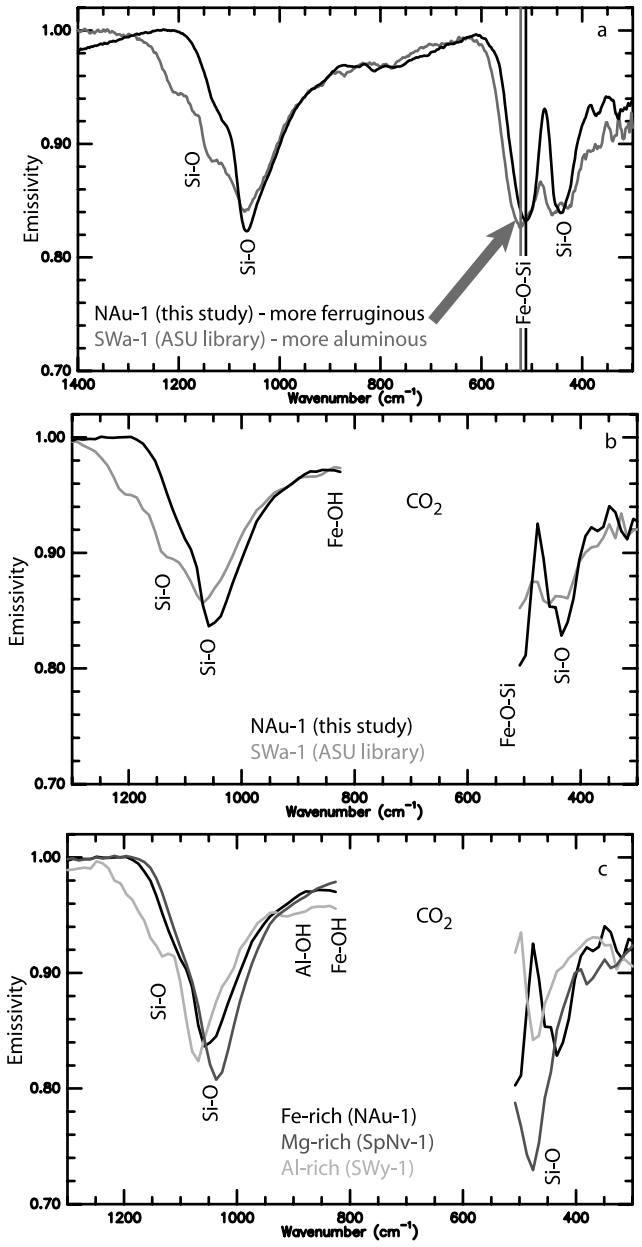

Figure 4. Thermal infrared emission spectra of two nontronite samples at (a) full laboratory spectral sampling (2 cm^{-1}) and (b) TES spectral sampling (10 cm^{-1}). The coarser spectral resolution of the TES instrument, compared to laboratory spectrometers, and the existence of atmospheric absorption features at Mars, limit the precision of crystal chemical assignments from TES data. See text for more discussion. Emission spectra of aluminous, magnesian, and ferruginous clays are compared at TES spectral sampling (Figure 4c). At TES sampling, major spectral groups of clay minerals can be identified (magnesian, aluminous, or ferruginous), but the dominant spectra features are related to tetrahedral (Si,Al)-O bonds.

minerals do not become oriented as a result of clay particle orientation.

3.4. Considerations for Remote Sensing of Mars

[20] The high spectral resolution of laboratory data allows precise qualitative assessments of crystal chemistry of clay minerals. For example, at the resolution of the laboratory spectrometer, the difference in the relative Fe-content of two nontronites can be determined by the placement of their M-O-Si absorptions near 510 cm^{-1}. TES spectra of Mars have slightly degraded spectral sampling (10 cm^{-1}) relative to laboratory data (2 cm^{-1}), and TES spectra from $\sim$500–800 cm^{-1} are dominated by atmospheric absorption. It would therefore be impossible to make precise interpretations of clay chemistry from TES spectra (e.g., the relative Fe-content of two nontronites) (Figure 4). However, the major spectral classes of clay minerals, Fe-, Al-, or Mg-rich, have spectral features that are different enough to be identified with TES-resolution spectra. Perhaps most importantly, the dominant spectral features of clay minerals at TES resolution are the absorptions related to (Si,Al)-O stretching and bending related to the tetrahedral sheets. This is fundamentally disconnected from the diagnostic spectral features clays in VNIR data, which are related to the M-OH and O-H absorptions in the octahedral sheets or H-O-H absorptions of interlayer water of clay minerals.

4. Emission Spectra of Clay-Bearing Rocks

[21] In this section, we discuss the spectral features of clay-bearing rocks (mudstones). We do not propose that the rocks presented here are a direct analog for expected Martian materials. However, these results demonstrate the principles involved in analysis of clay-bearing rocks with emission spectroscopy.

4.1. Qualitative Mineralogical Analysis of Clay-Bearing Rocks

[22] Analysis of the mudstone samples by XRD and thermal emission spectroscopy indicate that the samples are composed of quartz, alkali feldspars, and I/S clay minerals. Bulk powder XRD data of the mudstone samples indicate the presence of quartz, orthoclase, albite, and clay minerals. Analysis of oriented slide mounts of the <2 μm size fraction of the mudstones shows that the clay minerals are dominantly I/S mixed layer clay (though the degree of expandability is different for each sample). All of the mudstone spectra display absorptions between 950 and 1250 cm^{-1}, which indicate the presence of silicates with intermediate to high Si/O ratios (Figure 5). The most prominent absorptions observed in the shales correspond to the Si-O stretching of quartz, feldspar, and clay at 1200 cm^{-1}, 1049 cm^{-1}, and 1072 cm^{-1}, respectively. Al-O-Si absorptions corresponding to the illite-smectite phase are observed at 535 cm^{-1}. Al-OH deformation absorptions near 915 cm^{-1} are subtle, but present in the shale spectra. The placement of the Si-O stretching absorptions corresponding to the clay component suggest that the clay is dioctahedral with a moderate amount of Al^{3+} substituting for Si^{4+} in the tetrahedral sheet. The strong band at 535 cm^{-1} indicates that the clay component

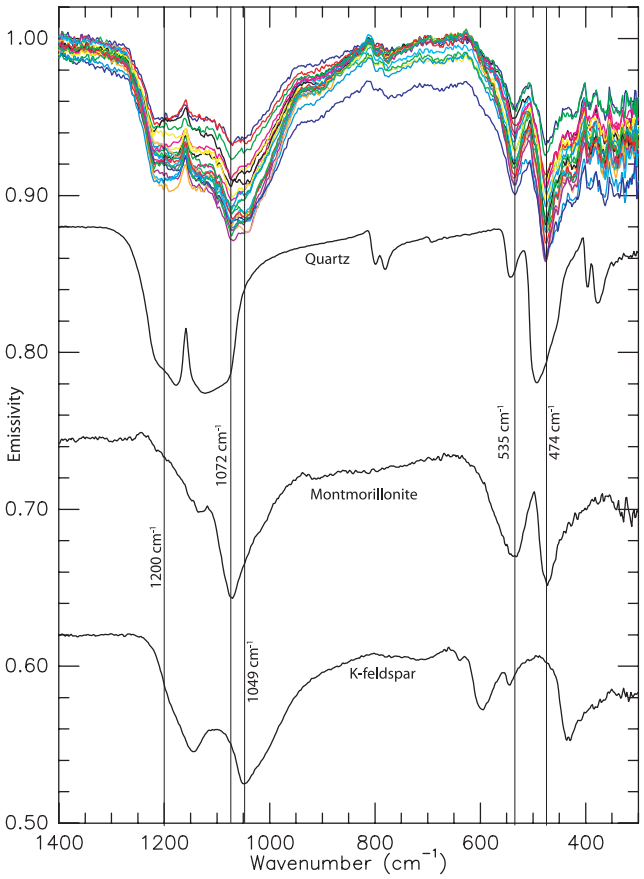

Figure 5. Thermal infrared emission spectra of all mudstone samples compared qualitatively with K-feldspar (orthoclase), montmorillonite, and quartz spectra. Specific absorptions are discussed in the text.

has an aluminous octahedral layer. Taken together, the qualitative inspection of these rock spectra suggests the presence of a clay component that is illite- or montmorillonite-like. The identification of quartz in the shale spectra is unambiguous. The presence of a silica phase is indicated by the strong absorption at 1200 cm^{-1}; that absorption, coupled with the local emissivity peak at 1160 cm^{-1}, cannot be explained by spectra of any other silica phases [*Michalski et al.*, 2003].

4.2. Quantitative Mineralogical Analysis of Clay-Bearing Rocks

[23] Quantification of mineral abundances in our mudstone samples by modeling of XRD data and modeling of thermal emission data are in general agreement (Figure 6). All of the mineral abundances reported here have been recast into volume modes. Quantitative analyses of random powder XRD mounts indicate that the mudstones are composed of 20–44% total clay minerals, 16–36% total feldspar, and 33–53% quartz, which is generally consistent with previous results [*Pytte*, 1982; *Lynch*, 1985; *Williams et al.*, 2001]. The average mineralogy of the mudstone samples determined by modeling of XRD data is 32% total clay, 27% total feldspar, and 41% quartz, with standard deviations of 6%, 5%, and 5%, respectively. Total abundances of modeled phases in rock samples using the XRD approach ranges from 95 to 104 wt%, which is an indication of relatively good model fits [*Środoń et al.*, 2001]. On the basis of linear spectral deconvolution of thermal emission spectra, the mudstone compositions range from 25 to 57% total clay minerals, 12 to 33% total feldspar, and 30 to 46% quartz. The average mineralogy of the mudstone samples determined by linear spectral deconvolution of thermal emission spectra is 39% total

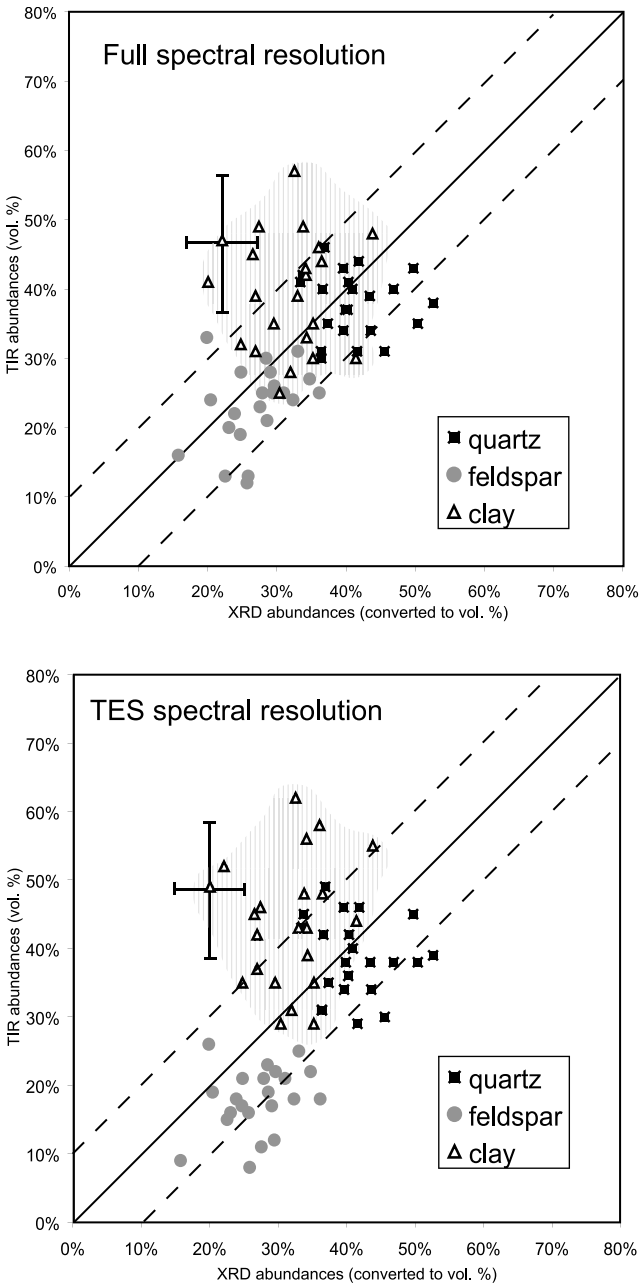

Figure 6. Scatterplots comparing the abundances of clay, feldspar, and quartz derived for mudstone samples by XRD modeling and spectral deconvolution of thermal infrared spectra. A one-to-one correlation line is shown for reference. The shaded area delineates the scatter in determination of clay mineral abundances. One error bar is shown for reference; errors are ±10% for infrared spectral deconvolution results and ±5% for XRD results.

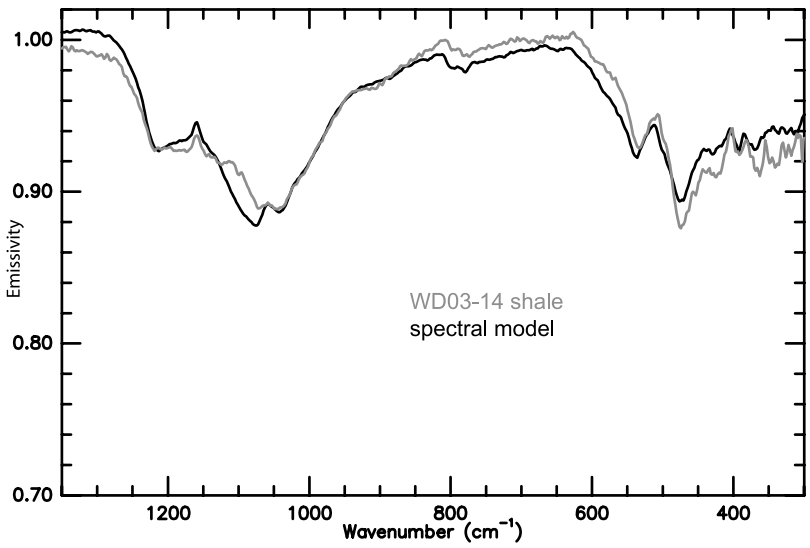

Figure 7. Thermal infrared emission spectrum of mudstone sample WD03-14 compared with the model spectrum from spectral deconvolution. Visually, there is a relatively poor fit between the spectra.

clay, 23% total feldspar, and 38% quartz, with standard deviations of 8%, 5%, and 6%, respectively.

[24] Despite the overall agreement between the average compositions of these rocks determined by both techniques, there are considerable differences in the abundance values in sample to sample comparisons (Figure 6). Some of the disagreement between abundance values determined by these two techniques should be attributed to the fact that comparisons are being made between two models, both of which have some intrinsic error. Errors associated with the XRD abundances are commonly <5% [*Środoń et al.*, 2001] and errors commonly associated with TIR spectral deconvolution are ~10% (for igneous and metamorphic rocks) [*Feely and Christensen*, 1999]. Some error associated with the modeling of both XRD and thermal emission data is attributable to compositional differences between the phases present in the rocks and the phases present in the respective libraries used for modeling. In addition, one might suspect some nonlinear spectral mixing of individual phases present in the mudstone samples. Petrologic inspection of the samples shows that clasts of quartz, feldspars, and clays are intimately mixed at scales of tens of μm, which could lead to photons interacting with multiple phases, multiply scattering, as they leave the rock surface. Visual inspection of some of the model spectra suggest relatively poor fits (Figure 7), which is an indication of potentially erroneous abundance values. However, despite the likelihood of some contribution of nonlinear mixing, the linear spectral deconvolution technique produces mineral abundances comparable to those determined by alternative techniques. If the rock spectra are resampled to the spectral resolution of the TES instrument, the results are relatively unchanged (Figure 6), which lends confidence to the use of this technique to analyze clay-bearing rocks with the TES data set. From this, we conclude that linear spectral deconvolution is a viable technique for estimation of clay mineral abundances in certain rock types, but we acknowledge that textural variations in different rock types could strongly bias the perceived abundance of clay minerals using this technique.

5. Application to TES Results

[25] The TES experiment has returned global thermal infrared spectra for Mars, which have been separated into atmospheric and surface components [*Bandfield et al.*, 2000; *Smith et al.*, 2000]. Surface emissivity spectra from 300–1600 cm^{-1} have been used to constrain the surface mineralogy of Mars, and *Bandfield et al.* [2000] determined that most of the spectral variability in Martian dark regions can be explained by combinations of two major spectral surface types: surface-type 1 (ST1) and surface-type 2 (ST2). The presence of broad absorptions between 850 and 1200 cm^{-1} provides definitive evidence of intermediate and mafic silicate materials on the Martian surface. Previous workers have demonstrated that qualitatively, ST1 is similar to spectra of some basaltic rocks (Deccan basalt, in particular) and ST2 is spectrally similar to andesitic rock from the Medicine Lake Caldera or to a weathered Columbia River Basalt [*Bandfield et al.*, 2000; *Wyatt and McSween*, 2002]. Because these two spectral shapes span most of the spectral variation of Martian dark regions, linear spectral deconvolution of these spectral shapes provides an approximation of the global-scale mineralogy of Martian dark regions.

5.1. Detection of Clay Minerals on Mars With TES

[26] Descriptions of the application of linear spectral deconvolution to analysis of TES data are provided by *Bandfield et al.* [2000], *Christensen et al.* [2000b], *Hamilton et al.* [2001], *Bandfield* [2002], *Rogers and Christensen* [2003], *Rogers et al.* [2005], and *Hamilton and Christensen* [2005]. All previous mineralogical interpretations from spectral deconvolution generally agree that equatorial dark regions of Mars (where ST1 is common) are dominated by plagioclase feldspar (33–55%) and clinopyroxene (25–41%); the precise mineral abundances

Table 2. Summary of Linear Spectral Deconvolution Results of TES Spectral Surface Types[a]

	JLB		VEH		MBW		HYM		This Study	
	ST1	ST2	ST1	ST2	ST1	ST2	ST1	ST2	ST1	ST2
Feldspar	50	35	55	49	33	39	35	18	49	43
Pyroxene	25	10	29	8	41	16	29	8	13	8
High silica	0	25	9	28	...	...	2	34	0	16
Clay minerals	15	15	5	8	14	31	22	18	22	15

[a]ST1, TES surface-type 1; ST2, TES surface-type 2; high silica, high-silica glass (78% SiO_2). JLB data are from *Bandfield et al.* [2000]. VEH data are from *Hamilton et al.* [2001]. MBW data are from *Wyatt and McSween* [2002] HYM data are from *McSween et al.* [2003].

depend on the spectral model used in each study. Many higher-latitude regions, including Acidalia Planitia and Vastitas Borealis (where ST2 is observed), have modeled mineralogies dominated by feldspars (18–49%) and a high-silica spectral component (25–34%).

[27] The mineralogical interpretation of the high-silica spectral component has been debated [*Bandfield et al.*, 2000; *Wyatt and McSween*, 2002; *Hamilton et al.*, 2002; *Minitti et al.*, 2002; *Morris et al.*, 2003; *Ruff*, 2003; *Kraft et al.*, 2003; *Wyatt et al.*, 2004; *Michalski et al.*, 2005]. Felsic volcanic glass (78 wt.% SiO_2) provides a reasonable spectral fit in modeling the ST2 spectra, which could indicate the widespread occurrence of primary felsic volcanic glasses on Mars. The high-silica component could also be explained by the occurrence of aluminous or ferric opaline silica or an intimate mixture of pure silica and other aluminosilicates (such as clay minerals or clay precursors) [*Kraft et al.*, 2003; *Michalski et al.*, 2005]. Abundances of felsic volcanic glasses and clay minerals derived from spectral deconvolution of TES data are sometimes grouped together [e.g., *Bandfield*, 2002], but are often reported separately [e.g., *Bandfield et al.*, 2000; *Hamilton et al.*, 2001; *McSween et al.*, 2003]. Recent spectral deconvolution analysis of mathematical spectral mixtures by *Koeppen and Hamilton* [2005] show that many high-silica materials and clay minerals can be distinguished on the basis of spectral deconvolution, provided that all phases present are included in the input library. It therefore seems reasonable to report abundances of high-silica phases and clay minerals separately.

[28] In addition to the high-silica spectral component, which may or may not include an admixture of clay minerals, past deconvolution results have yielded "sheet silicate" abundances (which probably do not include high-silica materials) ranging from 5 to 22% (Table 2). Reported abundances of sheet silicates are typically dominated by smectite clay minerals. The highest reported abundances of clay minerals from deconvolution of TES data is 31% [*Wyatt and McSween*, 2002]. However, in that study, *Wyatt and McSween* [2002] excluded felsic volcanic glass from the input library, which forced higher deconvolved abundances of clay minerals.

[29] We also used linear spectral deconvolution to model TES surface spectra and thereby estimate mineral abundances on the Martian surface, including the abundance of clay minerals. The analysis presented here differs from previous spectral deconvolution analyses of TES data primarily in that our spectra library contains newly acquired clay spectra in addition to typical igneous minerals. Previous researchers used clay mineral emission spectra acquired by *Piatek* [1997] and presented by *Christensen et al.* [2000a] in their analyses. We tested the hypothesis that the model results might be significantly different given a different suite of input clay mineral spectra. However, our spectral modeling results of global TES surface spectral types ST1 and ST2 are not significantly changed from those of previous authors [*Bandfield et al.*, 2000; *Hamilton et al.*, 2001; *Christensen et al.*, 2001; *Christensen et al.*, 2000b; *Wyatt and McSween*, 2002; *Bandfield*, 2002; *Rogers and Christensen*, 2003] (Table 2). ST1 can be modeled with a combination of feldspars (mostly andesine and labradorite), pyroxene (mostly augite), and clay minerals. ST2 can be well modeled with a combination of alkali and plagioclase feldspars, high-silica (Si/O > 0.4) material, and clay minerals. Modeled clay minerals (for ST1 and ST2) include halloysite, beidellite, and montmorillonite.

5.2. Geologic Implications of TES Detection of Clays

[30] The TES results provide evidence for modest abundances (~15–20%) of clay minerals in Martian dark regions, at the global scale. The fact that most reported analyses of TES spectra include abundances of clay minerals strongly suggests that the Martian surface has thermal infrared spectral characteristics that are clay-like. Although these clay abundances are only slightly above estimated detection limits, these observations should not be ignored; even rocks that are clay-rich by terrestrial standards, the mudstones, for example, may contain only 30% clay minerals. These abundances of clay minerals could have significant geologic meaning for the history of water on Mars.

[31] The possible detection of clay minerals with TES must be reconciled with the lack of detection of clay minerals, at global scales, using VNIR techniques [*Singer et al.*, 1979; *McCord et al.*, 1982; *Soderblom*, 1992; *Murchie et al.*, 1993; *Beinroth and Arnold*, 1996; *Bell et al.*, 1997; *Murchie et al.*, 2000; *Bibring et al.*, 2005; *Mustard et al.*, 2005]. Reconciliation of these seemingly conflicting results depends on understanding of the mineralogical meaning of the different spectral results. It is well known that VNIR spectra of clay minerals contain diagnostic absorptions related to O-H stretching of the octahedral sheets (at λ = 1.4 μm), H-O-H deformations related to interlayer water (at λ = 1.9 μm), and, perhaps most diagnostically, M-OH stretching absorptions related to the octahedral layer (at λ = 2.2–2.35 μm). Over the spectral range of the TES instrument, the relevant spectral features of clay minerals are predominantly absorptions corresponding to tetrahedral (Si,Al)-O stretching and bending modes (Figure 8). Detection of clay minerals using linear deconvolution of TES surface spectra is, fundamentally, detection of a material that (1) has an intermediate Si/O ratio (0.3–0.4), and (2) has limited spectral structure,

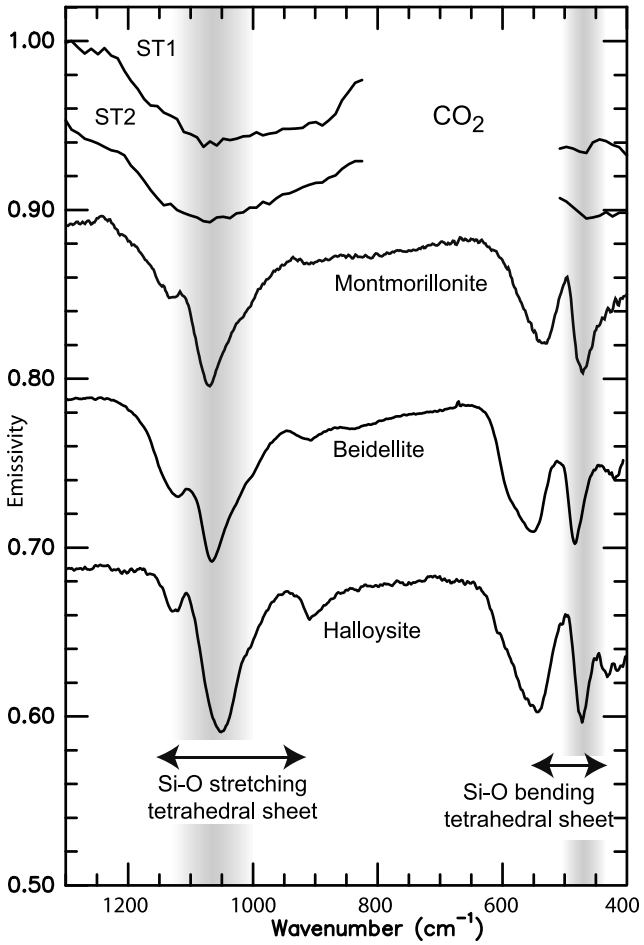

Figure 8. Qualitative comparison of the major Martian surface spectral types from TES [*Bandfield et al.*, 2000] with clay minerals. The spectral features of clay minerals that are modeled in spectral deconvolution of TES data are the absorptions corresponding to tetrahedral (Si,Al)-O bonds.

which is a reflection of limited crystalline ordering [*Parke*, 1974]. The TES detection of clay minerals is not directly tied to the hydration bands of clay minerals. In addition, the (Si,Al)-O spectral bands present in the thermal infrared are stronger spectral features than the hydration features present in the near-infrared (at λ = 1–2.35 μm).

[32] We propose that the spectrally clay-like materials detected by TES may correspond to aluminosilicate alteration materials present in Martian dark regions that are compositionally similar to clay minerals, but perhaps limited in their crystallinity and/or hydration state. Such materials could exist in several contexts that are plausible for Mars: (1) within immature sediments and sedimentary rocks, (2) within weathering rinds on volcanic rocks exposed at the surface, and (3) within rock or particle coatings. High-resolution imaging has shown that the Martian surface is nearly everywhere layered, suggesting that unconsolidated sediments and sedimentary rocks may cover significant portions of Mars [*Malin and Edgett*, 2000b, 2001]. Poorly crystalline aluminosilicate weathering products are common in immature sediments on Earth [*Weaver and Pollard*, 1973]. Such materials could exist as cements and grain coatings in immature sediments on Mars. Rocks exposed at the Martian surface may have weathering rinds and/or rock coatings. Textural [*McSween et al.*, 2004] and mineralogical [*Schröder et al.*, 2005] evidence for weathering rinds has been reported for basaltic rocks on the Martian surface at Gusev Crater. On Earth, poorly crystalline silicate weathering products occur as replacements of minerals or mesostatic phases in the rinds and as fracture fill in weathering rinds on volcanic rocks [*Colman*, 1982]. The presence of poorly crystalline silicate weathering products on Mars, in any of these contexts, indicates that aqueous alteration during their formation probably occurred in situations of relatively low water/rock ratios, or during wet conditions that were only episodic and transient. It is also possible that clay minerals formed earlier in Martian history have been oxidized at the surface, resulting in disruption of their octahedral sheets [*Burt*, 2002].

[33] If aluminosilicate weathering products occur on Mars, they must have formed by the chemical breakdown of igneous aluminosilicate starting materials. The presence of Al^{3+} in the weathering product implicates plagioclase or glass, in addition to pyroxenes or olivine, in the weathering process. The differential chemical breakdown of primary phases in Martian surface materials should affect igneous interpretations [e.g., *Bandfield et al.*, 2000; *Hamilton et al.*, 2001; *McSween et al.*, 2003] of remote sensing data [*Michalski et al.*, 2004].

6. Conclusions

[34] On the basis of our analysis of clay mineral standards and a suite of clay-bearing rocks, and consideration of Martian surface spectra from TES, we draw the following conclusions.

[35] 1. The mineralogical characteristics of clay minerals which are most important for remote geological studies using thermal emission spectra are (1) the Si/O ratio of the tetrahedral layer and (2) the major element chemistry of the octahedral layer (i.e., whether it is Mg-, Al-, or Fe-rich; and dioctahedral or trioctahedral). At high spectral resolution, differences in bulk chemistry of the octahedral sheets are observable. Trace element occurrences, interlayer cations, and interlayer water have no direct effect on the emission spectra of indurated clay minerals from 300–1700 cm^{-1}.

[36] 2. Linear spectral deconvolution can provide estimates of clay mineral abundances in fine-grained rocks, but the recovered mineral abundances are somewhat imprecise when the clay minerals are intimately mixed with other minerals.

[37] 3. TES spectra of Martian dark regions lack unequivocal evidence of widespread crystalline, indurated clay minerals. However, the incorporation of clay minerals into spectral deconvolution analyses of TES data could indicate that materials which are spectrally similar to clays (from 300–1300 cm^{-1}) are present on Mars. Because the most important spectral features of clays in this spectral range are Si-O stretching and bending features, spectrally similar material could include poorly crystalline aluminosilicates with Si/O ratios similar to clay minerals (Si/O = 0.3–0.4).

Such materials could be detectable on Mars with TES owing to their strong (Si,Al)-O vibrational absorptions, but go undetected by VNIR techniques, which are dependent on the materials hydration state and crystallinity.

[38] 4. The occurrence of a global spectral component (at high and low latitudes) of poorly crystalline aluminosilicate material with a clay-like composition indicates that much of the Martian surface is chemically weathered. Such materials could correspond to immature sedimentary materials, alteration products within weathering rinds on igneous rocks exposed at the surface, or thin coatings on surface rocks and rock particles.

[39] **Acknowledgments.** We would like to acknowledge Amanda Turner for excellent support in the capacity of research assistant, and Steven Ruff, Richard Morris, Douglas Ming, Trevor Graff, Paul Niles, Michael Wyatt, Amy Knudson, Timothy Glotch, Deanne Rogers, and Joshua Bandfield for discussions regarding TES results and spectroscopy of clay minerals. David Bish, an anonymous reviewer, and the Associate Editor provided thoughtful reviews that improved this manuscript. Funding for this work was provided in part by the Planetary Imaging and Analysis Facility and Advanced Training Institute grant 1230449 (P. R. C.), the Mars Fundamental Research Program (T. G. S.), U.S. Department of Energy grant DE-FG02-04ER15505 (L. B. W.), and NSF grant EAR-0229583 (L. B. W.).

References

Abrams, M. J., R. P. Ashley, L. C. Rowan, A. F. H. Goetz, and A. B. Kahle (1977), Mapping of hydrothermal alteration in the Cuprite mining district, Nevada, using aircraft scanner images for the spectral region 0.46 to 2.36 μm, *Geology*, *5*, 713–718.

Baker, V. R., M. H. Carr, V. C. Gulick, C. R. Williams, and M. S. Marley (1992), Channels and valley networks, in *Mars*, edited by H. H. Kieffer et al., pp. 493–522, Univ. of Ariz. Press, Tucson.

Bandfield, J. L. (2002), Global mineral distributions on Mars, *J. Geophys. Res.*, *107*(E6), 5042, doi:10.1029/2001JE001510.

Bandfield, J. L., V. E. Hamilton, and P. R. Christensen (2000), A global view of Martian surface compositions from MGS-TES, *Science*, *287*, 1626–1630.

Beinroth, A., and G. Arnold (1996), Analysis of weak surface absorption bands in the near-infrared spectra of Mars obtained by Phobos-2, *Vib. Spectrosc.*, *11*, 115–121.

Bell, J. F., M. J. Wolff, P. B. James, R. T. Clancy, S. W. Lee, and L. J. Martin (1997), Mars surface mineralogy from Hubble Space Telescope imaging during 1994–1995: Observations, calibration, and initial results, *J. Geophys. Res.*, *102*(E4), 9109–9123.

Bibring, J. P., et al. (2005), Mars surface diversity as revealed by the OMEGA/Mars Express observations, *Science*, *307*, doi:10.1126/science.1108806.

Bishop, J. L. (2002), The influence of octahedral and tetrahedral cation substitution on the structure of smectites and serpentines as observed through infrared spectroscopy, *Clay Miner.*, *37*, 617–628.

Bishop, J. L., C. M. Pieters, and R. G. Burns (1993), Reflectance and Mossbauer spectroscopy of ferrihydrite-montmorillonite assemblages as Mars soil analog materials, *Geochim. Cosmochim. Acta*, *57*(19), 4583–4595.

Bishop, J. L., C. M. Pieters, and J. O. Edwards (1994), Infrared spectroscopic analyses on the nature of water in montmorillonite, *Clays Clay Miner.*, *42*, 702–716.

Bishop, J. L., H. Froschl, and R. L. Mancinelli (1998), Alteration processes in volcanic soils and identification of exobiologically important weathering products on Mars using remote sensing, *J. Geophys. Res.*, *103*(E13), 31,457–31,476.

Bishop, J. L., S. L. Murchie, C. M. Pieters, and A. P. Zent (2002), A model for formation of dust, soil, and rock coatings on Mars: Physical and chemical processes on the Martian surface, *J. Geophys. Res.*, *107*(E11), 5097, doi:10.1029/2001JE001581.

Borden, D., and R. F. Giese (2001), Baseline studies of the Clay Minerals Society source clays: Cation exchange capacity measurements by the ammonia electrode method, *Clays Clay Miner.*, *49*, 444–445.

Brindley, G. W., and J. Zussman (1959), Infra-red absorption data for serpentine minerals, *Am. Mineral.*, *44*, 185–189.

Burt, D. M. (2002), Hydrogen loss in iron-bearing Mars clays (or palagonite) is oxidation, not "dehydroxylation," *Lunar Planet. Sci.*, *XXVI*, abstract 1242.

Carr, M. H. (1996), *Water on Mars*, 229 pp., Oxford Univ. Press, New York.

Chapman, M. G. (2003), Layered, massive and thin sediments on Mars: Possible Late Noachian to Early Amazonian tephra, in *Volcano-Ice Interaction on Earth and Mars*, edited by J. L. Smellie and M. Chapman, pp. 273–294, Geol. Soc. of London, London.

Chipera, S. J., and D. L. Bish (2001), Baseline studies of the Clay Minerals Society source clays: Powder X-ray diffraction analyses, *Clays Clay Miner.*, *49*, 398–409.

Christensen, P. R. (2003), Formation of recent Martian gullies through melting of extensive water-rich snow deposits, *Nature*, *422*, 45–48.

Christensen, P. R., and S. T. Harrison (1993), Thermal infrared emission spectroscopy of natural surfaces: Application to desert varnish coatings on rocks, *J. Geophys. Res.*, *98*(B11), 19,819–19,834.

Christensen, P. R., J. L. Bandfield, M. D. Smith, V. E. Hamilton, and R. N. Clark (2000a), Identification of a basaltic component on the Martian surface from Thermal Emission Spectrometer data, *J. Geophys. Res.*, *105*(E4), 9609–9621.

Christensen, P. R., J. L. Bandfield, V. E. Hamilton, D. A. Howard, M. D. Lane, J. L. Piatek, S. W. Ruff, and W. L. Stefanov (2000b), A thermal emission spectral library of rock-forming minerals, *J. Geophys. Res.*, *105*(E4), 9735–9739.

Christensen, P. R., et al. (2001), Mars Global Surveyor Thermal Emission Spectrometer experiment: Investigation description and surface science results, *J. Geophys. Res.*, *106*(E10), 23,823–23,871.

Colman, S. (1982), Chemical weathering of basalts and andesites: Evidence from weathering rinds, *U.S. Geol. Surv. Prof. Pap.*, *1246*, 51 pp.

Eberl, D. D. (2003), User's guide to Rockjock—A program for determining quantitative mineralogy from powder X-ray diffraction data, *U.S. Geol. Surv. Open File Rep., 03-78*, 42 pp.

Eberl, D. D., B. F. Jones, and H. N. Khoury (1982), Mixed-layer kerolite/stevensite from the Amargosa Desert, Nevada, *Clays Clay Miner.*, *30*, 321–326.

Edgett, K. S., and M. C. Malin (2002), Martian sedimentary rock stratigraphy: Outcrops and interbedded craters of northwest Sinus Meridiani and southwest Arabia Terra, *Geophys. Res. Lett.*, *29*(24), 2179, doi:10.1029/2002GL016515.

Fagents, S. A., P. Lanagan, and R. Greeley (2003), Rootless cones on Mars: A consequence of lava-ground ice interaction, in *Volcano-Ice Interaction on Earth and Mars*, edited by J. L. Smellie and M. Chapman, pp. 295–318, Geol. Soc. of London, London.

Farmer, V. C. (1958), The infra-red spectra of talc, saponite, and hectorite, *Mineral. Mag.*, *31*, 829–845.

Farmer, V. C. (1974), The layer silicates, in *The Infrared Spectra of Minerals*, edited by V. C. Farmer, pp. 331–363, Mineral. Soc., London.

Farmer, V. C., and J. D. Russell (1964), The infra-red spectra of layer silicates, *Spectrochim. Acta*, *20*, 1149–1173.

Feely, K. C., and P. R. Christensen (1999), Quantitative compositional analysis using thermal emission spectroscopy: Application to igneous and metamorphic rocks, *J. Geophys. Res.*, *104*(E10), 24,195–24,210.

Feldman, W. C., et al. (2002), Global distribution of neutrons from Mars: Results from Mars Odyssey, *Science*, *297*, 75–78.

Feldman, W. C., et al. (2004), Global distribution of near-surface hydrogen on Mars, *J. Geophys. Res.*, *109*, E09006, doi:10.1029/2003JE002160.

Fialips, C. I., J. W. Carey, D. T. Vaniman, D. L. Bish, W. C. Feldman, and M. T. Mellon (2005), Hydration state of zeolites, clays, and hydrated salts under present-day Martian surface conditions: Can hydrous minerals account for Mars Odyssey observations of near-equatorial water-equivalent hydrogen?, *Icarus*, *178*, 74–83.

Gates, W. P. (2005), Infrared spectroscopy and the chemistry of dioctahedral smectites, in *The Application of Vibrational Spectroscopy to Clay Minerals and Layered Double Hydroxides*, *CMS Workshop Lectures*, vol. 13, edited by J. T. Kloprogge, pp. 125–168, Clay Miner. Soc., Aurora, Colo.

Goetz, A. F. H., B. N. Rock, and L. C. Rowan (1983), Remote sensing for exploration: An overview, *Econ. Geol.*, *78*, 573–590.

Gooding, J. L., R. E. Arvidson, and M. Y. Zolotov (1992), Physical and chemical weathering, in *Mars*, edited by H. H. Kieffer et al., pp. 626–651, Univ. of Ariz. Press, Tucson.

Guggenheim, S., and A. F. Koster Van Groos (2001), Baseline studies of the Clay Minerals Society source clays: Thermal analysis, *Clays Clay Miner.*, *49*, 433–443.

Hamilton, V. E., and P. R. Christensen (2005), Evidence for extensive, olivine-rich bedrock on Mars, *Geology*, *33*, 433–436.

Hamilton, V. E., P. R. Christensen, and H. Y. J. McSween (1997), Determination of Martian meteorite lithologies and mineralogies using vibrational spectroscopy, *J. Geophys. Res.*, *102*(E11), 25,593–25,603.

Hamilton, V. E., M. B. Wyatt, H. Y. J. McSween, and P. R. Christensen (2001), Analysis of terrestrial and Martian volcanic compositions using thermal emission spectroscopy: 2. Application to Martian surface spectra

from the Mars Global Surveyor Thermal Emission Spectrometer, *J. Geophys. Res.*, *106*(E7), 14,733–14,746.
Hamilton, V. E., P. R. Christensen, and J. L. Bandfield (2002), Volcanism or aqueous alteration on Mars?, *Nature*, *421*, 711–712.
Hower, J., and T. C. Mowatt (1966), The mineralogy of illites and mixed-layer illite/montmorillonites, *Am. Mineral.*, *51*, 825–854.
Hunt, G. R., and R. P. Ashley (1979), Spectra of altered rocks in the visible and near infrared, *Econ. Geol.*, *74*, 1613–1629.
Hunt, G. R., and R. C. Evarts (1981), The use of near-infrared spectroscopy to determine the degree of serpentinization of ultramafic rocks, *Geophysics*, *46*(3), 316–321.
Hunt, G. R., and R. B. Hall (1981), Identification of kaolins and associated minerals in altered volcanic rocks by infrared spectroscopy, *Clays Clay Miner.*, *29*, 76–78.
Hunt, G. R., and J. W. Salisbury (1970), Visible and near-infrared spectra of minerals and rocks: I. Silicate minerals, *Mod. Geol.*, *1*, 283–300.
Hunt, G. R., J. W. Salisbury, and C. J. Lenhoff (1973), Visible and near infrared spectra of minerals and rocks: VI. Additional silicates, *Mod. Geol.*, *4*, 85–106.
Keeling, J. L., M. D. Raven, and W. P. Gates (2000), Geology and characterization of two hydrothermal nontronites from weathered metamorphic rocks at the Uley graphite mine, south Australia, *Clays Clay Miner.*, *48*, 537–548.
Keeling, J. L., M. D. Raven, and W. P. Gates (2001), Geology and characterization of two hydrothermal nontronites from weathered metamorphic rocks at the Uley graphite mine, south Australia, *Clays Clay Miner.*, *48*, 537–548.
Keller, W. D., and E. E. Pickett (1950), Absorption of infra-red radiation by clay minerals, *Am. J. Sci.*, *248*, 264–273.
Khoury, H. N., D. D. Eberl, and B. F. Jones (1982), Origin of magnesium clays from the Amargosa Desert, Nevada, *Clays Clay Miner.*, *30*, 327–336.
Kloprogge, J. T., and R. L. Frost (2005), Infrared emission spectroscopy of clay minerals, in *The Application of Vibrational Spectroscopy to Clay Minerals and Layered Double Hydroxides*, *CMS Workshop Lectures*, vol. 13, edited by J. T. Kloprogge, pp. 65–98, Clay Miner. Soc., Aurora, Colo.
Kloprogge, J. T., R. L. Frost, and L. Hickey (2000), Infrared emission spectroscopic study of dehydroxylation of some smectites, *Thermochim. Acta*, *345*, 145–156.
Koeppen, W. C., and V. E. Hamilton (2005), Discrimination of glass and phyllosilicates minerals in thermal infrared data, *J. Geophys. Res.*, *110*, E08006, doi:10.1029/2005JE002474.
Kogel, J. E., and S. A. Lewis (2001), Baseline studies of the Clay Minerals Society source clays: Chemical analysis by inductively coupled plasma mass spectroscopy (ICP-MS), *Clays Clay Miner.*, *49*, 387–392.
Kraft, M. D., J. R. Michalski, and T. G. Sharp (2003), Effects of pure silica coatings on thermal emission spectra of basaltic rocks: Considerations for Martian surface mineralogy, *Geophys. Res. Lett.*, *30*(24), 2288, doi:10.1029/2003GL018848.
Lang, H. R., M. J. Bartholomew, C. I. Grove, and E. D. Paylor (1990), Spectral reflectance characterization (0.4 to 2.5 and 8.0 to 12.0 μm) of Phanerozoic strata, Wind River Basin and southern Bighorn Basin areas, Wyoming, *J. Sediment. Petrol.*, *60*(4), 504–524.
Launer, P. J. (1952), Regularities in the infra-red spectra of silicate minerals, *Am. Mineral.*, *37*, 764–784.
Lynch, F. L., III (1985), The stoichiometry of the smectite to illite reaction in a contact metamorphic environment, M.S. thesis, 84 pp., Dartmouth College, Hanover, N. H.
Madejová, J. (2003), FTIR techniques in clay mineral studies, *Vib. Spectrosc.*, *31*, 1–10.
Madejová, J., and P. Komadel (2001), Baseline studies of the Clay Minerals Society source clays: Infrared methods, *Clays Clay Miner.*, *49*, 410–432.
Madejová, J., and P. Komadel (2005), Information available from infrared spectra of the fine fractions of bentonites, in *The Application of Vibrational Spectroscopy to Clay Minerals and Layered Double Hydroxides*, *CMS Workshop Lectures*, vol. 13, edited by J. T. Kloprogge, pp. 65–98, Clay Miner. Soc., Aurora, Colo.
Malin, M. C., and K. S. Edgett (2000a), Evidence for recent groundwater seepage and surface runoff on Mars, *Science*, *288*, 2330–2335.
Malin, M. C., and K. S. Edgett (2000b), Sedimentary rocks of early Mars, *Science*, *290*, 1927–1937.
Malin, M. C., and K. S. Edgett (2001), Mars Global Surveyor Mars Orbiter Camera: Interplanetary cruise through primary mission, *J. Geophys. Res.*, *106*(E10), 23,429–23,570.
Malin, M. C., and K. S. Edgett (2003), Evidence for persistent flow and aqueous sedimentation on early Mars, *Science*, *302*, 1931–1934.
McCord, T. B., R. L. Clark, and R. B. Singer (1982), Mars: Near-infrared spectral reflectance of surface regions and compositional implications, *J. Geophys. Res.*, *87*(B4), 3021–3032.
McSween, H. Y. J., T. L. Grove, and M. B. Wyatt (2003), Constraints on the composition and petrogenesis of the Martian crust, *J. Geophys. Res.*, *108*(E12), 5135, doi:10.1029/2003JE002175.
McSween, H. Y. J., et al. (2004), Basaltic rocks analyzed by the Spirit Rover in Gusev Crater, *Science*, *305*, 842–845.
Mermut, A. R., and A. F. Cano (2001), Baseline studies of the Clay Minerals Society source clays: Chemical analyses of major elements, *Clays Clay Miner.*, *49*, 381–386.
Michalski, J. R., M. D. Kraft, T. Diedrich, T. G. Sharp, and P. R. Christensen (2003), Thermal emission spectroscopy of the silica polymorphs and considerations for remote sensing of Mars, *Geophys. Res. Lett.*, *30*(19), 2008, doi:10.1029/2003GL018354.
Michalski, J. R., S. J. Reynolds, T. G. Sharp, and P. R. Christensen (2004), Thermal infrared analysis of weathered granitic rock compositions in the Sacaton Mountains, Arizona: Implications for petrologic classifications from thermal infrared remote-sensing, *J. Geophys. Res.*, *109*, E03007, doi:10.1029/2003JE002197.
Michalski, J. R., M. D. Kraft, T. G. Sharp, L. B. Williams, and P. R. Christensen (2005), Mineralogical constraints on the high-silica Martian surface component observed by TES, *Icarus*, *174*, 161–177.
Minitti, M. E., J. F. Mustard, and M. J. Rutherford (2002), The effects of glass content and oxidation on the spectra of SNC-like basalts: Applications to Mars remote sensing, *J. Geophys. Res.*, *107*(E5), 5030, doi:10.1029/2001JE001518.
Moll, W. F. (2001), Baseline studies of the Clay Minerals Society source clays: Geological origin, *Clays Clay Miner.*, *49*, 374–380.
Moore, D. M., and R. C. Reynolds Jr. (1997), *X-Ray Diffraction and the Identification and Analysis of Clay Minerals*, 378 pp., Oxford Univ. Press, New York.
Morris, R. V., T. G. Graff, S. A. Mertzman, M. D. Lane, and P. R. Christensen (2003), Palagonitic (not andesitic) Mars: Evidence from thermal emission and VNIR spectra of palagonitic alteration rinds on basaltic rock, paper presented at Sixth International Conference on Mars, Lunar Planet. Inst., Pasadena, Calif.
Murchie, S. L., J. F. Mustard, J. L. Bishop, J. W. Head, C. M. Pieters, and S. Erard (1993), Spatial variations in the spectral properties of bright regions on Mars, *Icarus*, *105*, 454–468.
Murchie, S. J., L. Kirkland, S. Erard, J. Mustard, and M. Robinson (2000), Near-infrared spectral variations of Martian surface materials from ISM imaging spectrometer data, *Icarus*, *147*, 444–471.
Mustard, J. F., and C. M. Pieters (1987), Abundance and distribution of ultramafic microbreccia in Moses Rock dike: Quantitative application of mapping spectroscopy, *J. Geophys. Res.*, *92*(B10), 10,376–10,390.
Mustard, J. F., C. D. Cooper, and M. K. Rifkin (2001), Evidence of recent climate change on Mars from the identification of youthful near-surface ground ice, *Nature*, *412*(6845), 411–414.
Mustard, J. F., et al. (2005), Crustal formation, volcanism, and alteration in the Syrtis Major region revealed by OMEGA data, *Lunar Planet. Sci.* [CD-ROM], *XXXVI*, abstract 1341.
Parke, S. (1974), Glasses, in *The Infrared Spectra of Minerals*, edited by V. C. Farmer, pp. 483–514, Mineral. Soc., London.
Petit, S. (2005), Crystal chemistry of talcs: A NIR and MIR spectroscopic approach, in *The Application of Vibrational Spectroscopy to Clay Minerals and Layered Double Hydroxides*, *CMS Workshop Lectures*, vol. 13, edited by J. T. Kloprogge, pp. 65–98, Clay Miner. Soc., Aurora, Colo.
Piatek, J. L. (1997), Vibrational spectroscopy of clay minerals: Implications for remote sensing of terrestrial planetoids, M.S. thesis, 75 pp., Ariz. State Univ., Tempe.
Post, J. L., B. L. Cupp, and F. T. Madsen (1997), Beidellite and associated clays from the DeLamar Mine and Florida Mountain area, *Clays Clay Miner.*, *45*, 240–250.
Pytte, A. M. (1982), The kinetics of the smectite to illite reaction in contact metamorphic shales, M.A. thesis, 78 pp., Dartmouth College, Hanover, N. H.
Ramsey, M. S., and P. R. Christensen (1998), Mineral abundance determination: Quantitative deconvolution of thermal emission spectra, *J. Geophys. Res.*, *103*(B1), 577–596.
Rogers, D., and P. R. Christensen (2003), Age relationship of basaltic and andesitic surface compositions on Mars: Analysis of high-resolution TES observations of the Northern Hemisphere, *J. Geophys. Res.*, *108*(E4), 5030, doi:10.1029/2002JE001913.
Rogers, A. D., P. R. Christensen, and J. L. Bandfield (2005), Compositional heterogeneity of the ancient Martian crust: Analysis of Ares Vallis bedrock with THEMIS and TES data, *J. Geophys. Res.*, *110*, E05010, doi:10.1029/2005JE002399.
Roush, T., and J. B. Orenberg (1996), Estimated detectability limits of iron-substituted montmorillinite clay on Mars from thermal emission spectra of clay-palagonite physical mixtures, *J. Geophys. Res.*, *101*(E11), 26,111–26,118.

Ruff, S. W. (1998), Quantitative thermal emission spectroscopy applied to granitoid petrology, Ph.D. dissertation, 234 pp., Ariz. State Univ., Tempe.

Ruff, S. W. (2003), Basaltic andesite or weathered basalt: A new assessment, paper presented at Sixth International Conference on Mars, Lunar Planet. Inst., Pasadena, Calif.

Ruff, S. W., P. R. Christensen, P. W. Barbera, and D. L. Anderson (1997), Quantitative thermal emission spectroscopy of minerals: A laboratory technique for measurement and calibration, *J. Geophys. Res.*, *102*(B7), 14,899–14,913.

Schröder, C., G. Klingelhöfer, R. V. Morris, D. S. Rodionov, P. A. de Souza, D. W. Ming, A. S. Yen, R. Gellert, and J. W. Bell III (2005), Weathering of basaltic rocks from the Gusev plains up to the Columbia Hills from the perspective of the MER Mössbauer spectrometer, *Lunar Planet Sci.* [CD-ROM], *XXXVI*, abstract 2309.

Singer, R. B., T. B. McCord, R. L. Clark, J. B. Adams, and R. L. Huguenin (1979), Mars surface composition from reflectance spectroscopy: A summary, *J. Geophys. Res.*, *84*(B14), 8415–8426.

Smith, M. D., J. L. Bandfield, and P. R. Christensen (2000), Separation of atmospheric and surface spectral features in Mars Global Surveyor Thermal Emission Spectrometer (TES) spectra, *J. Geophys. Res.*, *105*(E4), 9589–9607.

Soderblom, L. A. (1992), The composition and mineralogy of the Martian surface from spectroscopic observations: 0.3 mm to 50 mm, in *Mars*, edited by H. H. Kieffer et al., pp. 557–593, Univ. of Ariz. Press, Tucson.

Squyres, S. W., S. M. Clifford, R. O. Kuzmin, J. R. Zimbelman, and F. M. Costard (1992), Ice in the Martian regolith, in *Mars*, edited by H. H. Kieffer et al., pp. 523–554, Univ. of Ariz. Press, Tucson.

Squyres, S. W., et al. (2004), The Opportunity Rover's Athena science investigation at Meridiani Planum, Mars, *Science*, *306*, 1698–1703.

Środoń, J., V. A. Drits, D. K. McCarty, J. C. C. Hsieh, and D. D. Eberl (2001), Quantitative X-ray diffraction analysis of clay-bearing rocks from random preparations, *Clays Clay Miner.*, *49*, 514–528.

Stefanov, W. L. (2000), Investigation of hillslope processes and land cover change using remote sensing and laboratory spectroscopy, Ph.D. thesis, 250 pp., Ariz. State Univ., Tempe.

Stubican, V., and R. Roy (1961a), A new approach to assignment of infrared absorption bands in layer-silicate structures, *Z. Kristallogr.*, *115*, 200–214.

Stubican, V., and R. Roy (1961b), Isomorphous substitution and infrared spectra of the layer lattice silicates, *Am. Mineral.*, *46*, 32–51.

Tanaka, K. L., J. A. Skinner Jr., T. M. Hare, T. Joyal, and A. Wenker (2003), Resurfacing history of the northern plains of Mars based on geologic mapping of Mars Global Surveyor data, *J. Geophys. Res.*, *108*(E4), 8043, doi:10.1029/2002JE001908.

Weaver, C. E., and L. D. Pollard (1973), *The Chemistry of Clay Minerals*, 213 pp., Elsevier, New York.

Wenju, W. (2001), Baseline studies of the Clay Minerals Society source clays: Colloid and surface phenomena, *Clays Clay Miner.*, *49*, 446–452.

Williams, L. B., R. L. Hervig, and I. Hutcheon (2001), Boron isotope geochemistry during diagenesis: Part II. Application to organic-rich sediments, *Geochim. Cosmochim. Acta*, *65*(11), 1783–1794.

Wyatt, M. B., and H. Y. J. McSween (2002), Spectral evidence for weathered basalt as an alternative to andesite in the northern lowlands of Mars, *Nature*, *417*, 263–266.

Wyatt, M. B., V. E. Hamilton, H. Y. J. McSween, P. R. Christensen, and L. A. Taylor (2001), Analysis of terrestrial and Martian volcanic compositions using thermal emission spectroscopy: 1. Determination of mineralogy, chemistry, and classification strategies, *J. Geophys. Res.*, *106*(E7), 14,711–14,732.

Wyatt, M. B., H. Y. McSween Jr., K. L. Tanaka, and J. W. Head III (2004), Global geologic context for rock types and surface alteration on Mars, *Geology*, *32*, 644–648.

P. R. Christensen, M. D. Kraft, J. R. Michalski, T. G. Sharp, and L. B. Williams, Department of Geological Sciences, Arizona State University, Box 1404, Tempe, AZ 85287-1404, USA. (michalski@asu.edu)